

# Prediction Model of Gas Quantity Emitted from Coal Face Based on PCA-GA-BP Neural Network and Its Application

J. W. Qiu<sup>a, b, \*</sup>, Z. G. Liu<sup>a, b</sup>, L. Zhou<sup>a, b</sup>, R. X. Qin<sup>a, c</sup>

<sup>a</sup>School of Mining and Safety Engineering, Anhui University of Science and Technology, Huainan Anhui 232001, China;

<sup>b</sup>Key Laboratory of Safety and High-efficiency Coal Mining, Ministry of Education, Anhui University of Science and Technology, Huainan, 232001, China;

<sup>c</sup>Faculty of Mining and Geoengineering, AGH University of Science and Technology, Krakow 30-059, Poland

## Abstract

Gas has always been a serious hidden danger in coal mining. The quantity of gas emitted from the coal face is affected by many factors. To overcome the difficulty in accurately predicting the quantity of emission, a novel predictive model (PCA-GA-BP) based on principal component analysis (PCA), genetic algorithm (GA) and back propagation (BP) neural network was proposed. The model was tested and applied in different coal seams at Panbei Coal Mine in Huainan, China, involving sixteen training samples and four predicting samples. Results showed that: Gas emission quantity was significantly correlated with burial depth, gas content in the mining layer, gas content in the adjacent layer, and layer spacing. The correlations among these variables exceeded 60%. Linear regression analysis using the optimized model was affected by sample size and discreteness. The correlation coefficient (R) and maximum relative error (MRE) of the PCA-GA-BP model were 0.9988 and 3.02%, respectively. The MRE of the optimized model was 70.2% and 53.2% smaller than that of the BP and GA-BP models, respectively. The conclusions obtained in the study provide technical support for the prediction of gas quantity emitted from coal face, and the proposed method can be used in other engineering fields.

**Keywords:** Principal component analysis; Genetic algorithm; BP neural network; Gas emission; Prediction

## 1. Introduction

Gas is a major threat to the safety of coal miners and a significant research topic in mining engineering [10]. Coal mine gas disasters in China are a recurrent problem. Gas disasters account for more than 80% of the total coal mine accidents and 90% of the total number of coal mine casualties [16]. Gas content, one of the basic parameters in gas emission and gas outburst prediction, plays an important role in the prediction and prevention of coal mine fire and gas disasters. Precise prediction of gas content is of practical significance in mine ventilation design and production safety. Therefore, quick and accurate prediction of mine gas has become a crucial research topic.

The quantity of gas emitted from the coal face is affected by natural, geological, and mining factors. No theory can perfectly establish the relationships among these factors, because of the complex nonlinear relations among them. Therefore, studying the complex relationships among the factors that affect gas emission is a challenge. Prediction of

gas emission quantity is an intricate and continuously changing process. Currently, two methods are used to predict gas emission quantity: linear and nonlinear prediction. Traditional methods mostly involve linear prediction based on a mathematical model. However, with the change in geological conditions, a nonlinear prediction method that is suitable for complex conditions needs to be established. In recent years, intelligent algorithms have been proposed for nonlinear prediction, but these algorithms present disadvantages when used in isolation. As a result, the accuracy of the prediction cannot be guaranteed. A combination of several algorithms to improve prediction accuracy is widely seen as a smart development going forward.

This study analyzes the basic principles and characteristics of three algorithms, namely, principal component analysis (PCA), back propagation (BP) neural network, and genetic algorithm (GA), and proposes a novel coupled prediction method for improving the precision of prediction.

## 2. State of the art

Many researchers worldwide have conducted studies on predicting the quantity of gas emitted from the coal face.

\*Corresponding author

Email address: jwqiu2000@163.com (J. W. Qiu<sup>a, b, \*</sup>)

They have proposed many nonlinear prediction models and approaches based on regression analysis, fuzzy comprehensive evaluation method, nonlinear reflection method, and suchlike. Lv [3] emphasized the mutual impact of prediction indexes and proposed a prediction method combining PCA and multi-step linear regression analysis for the gas quantity emitted from the coal face. The method can reduce the number of variables, but the established model is intricate, and the nonlinear relationship among variables is ignored. Bai and Zhu [23, 24] considered the uncertain relationships among complex factors and developed a prediction model of gas emission quantity based on the artificial neural network. The results of the prediction with the artificial neural network were more precise than those obtained through linear regression. However, the prediction model of the traditional artificial neural network possesses low convergence speed and easily falls into the local optimal solution. Wang [19] presented an immune neural network prediction model based on the immune algorithm and the neural network for the prediction of gas concentration on the coal face. Furthermore, Yan [22] presented a back propagation (BP) neural network model based on the immune genetic algorithm. The two models can overcome the limitations of the traditional BP neural network, but cannot solve the issues of mutual effects generated by information overlays among the predictive indices. Liu and Wei [5, 21] proposed a grey theory model for forecasting the gas emission quantity in coal mines. The advantages of the grey theory model are: minimal input data, simple calculation, and high precision. However, the grey model does not consider the relationships among different factors and is largely dependent on historical data. Wang [20] proposed a fresh approach based on virtual state variables and the Kalman filter, and developed a gas emission quantity prediction model based on the Kalman filter algorithm. The method has the potential to deal with the uncertainty of fuzzy clustering analysis and deliver multi-index quantitative prediction. However, a large amount of previous sample data is required in the prediction. Ohga [11] adopted the simulator “COALGAS” for the prediction of gas emission. Furthermore, Saghafi [14] presented a tier 3 approach for estimating fugitive gas emission from surface coal mining. The new method was applied to an active Australian open coal mine. In this method, a mathematical model needs to be established and an appropriate mathematical method must be selected for the prediction of gas emission quantity. If the established mathematical model and the selected estimation method are unreasonable, large errors would be produced.

These prediction methods have contributed greatly to the prediction of gas emission quantity, but they all possess limitations. To solve the problem of the mutual influence of forecasting indices, the information of the gas emission prediction index was abstracted in this study and multiple associated and overlapping variables were transformed into an independent comprehensive component index by using PCA theory. GA and BP neural network were combined to improve the weights and thresholds and optimize the local

search and adaptive abilities of the BP neural network as well as to enhance the prediction precision of the model. PCA, BP neural network, and GA were merged to develop a prediction model called PCA-GA-BP. The model possesses high prediction precision and fast convergence rate.

The remainder of this paper is organized as follows: Section 3 provides a description of PCA and the GA-BP neural network algorithm and presents the prediction model of gas emission quantity based on the PCA-GA-BP neural network. Section 4 shows the application of the model and discusses the applicability of the method through a practical case. Section 5 presents a summary of the entire paper and the relevant conclusions.

### 3. Methodology

#### 3.1. PCA algorithm

PCA [12, 18, 15] is a technology for data compression and feature information extraction. In data processing, high-dimensional data sets are often encountered, and because of the high dimensionality of the data and the presence of many variables, correlations exist among the variables. Therefore, sample data do not completely reflect the main information of the total data. When statistical methods are used to study multivariate problems, too many variables can affect the computational load and increase the analytical complexity. PCA is based on the projection method. High-dimensional data can be projected into a low-dimensional space, such that the dimension of the data is reduced and the data structure is simplified. During simplification, PCA is used to deal with the related variables with as little information loss as possible.

##### 3.1.1. Mathematical model of PCA

Suppose that  $n$  samples, including  $p$  variables  $x_1, x_2, \dots, x_p$ , exist. The original data matrix of samples is expressed as follows:

$$X = \begin{bmatrix} x_{11} & x_{12} & \cdots & x_{1p} \\ x_{21} & x_{22} & \cdots & x_{2p} \\ \vdots & \vdots & \ddots & \vdots \\ x_{n1} & x_{n2} & \cdots & x_{np} \end{bmatrix} \quad (1)$$

$P$  variables of original data matrix  $x$  compose a linear combination  $F = AX$ , and  $p$  new comprehensive variables are obtained, namely,

$$\begin{cases} F_1 = a_{11}x_1 + a_{12}x_2 + \dots + a_{1p}x_p \\ F_2 = a_{21}x_1 + a_{22}x_2 + \dots + a_{2p}x_p \\ \dots \\ F_p = a_{p1}x_1 + a_{p2}x_2 + \dots + a_{pp}x_p \end{cases} \quad (2)$$

The model must meet the following conditions [17].

1.  $F_i$  and  $F_j$  are not related to each other ( $i \neq j, i, j = 1, 2, \dots, p$ ).
2.  $Var(F_1) \geq Var(F_2) \geq \dots \geq Var(F_p)$ , the importance of the principal component diminishes.
3.  $a_{k1}^2 + a_{k2}^2 + \dots + a_{kp}^2 = 1, k = 1, 2, \dots, p$

### 3.1.2. Solution of principal components

The solution of principal components involves computing transformation matrix  $A$ . The steps to solve the principal components are as follows.

**Step 1:** The original data are standardized, and the covariance matrix between variables is calculated.

**Step 2:** The eigenvalues of covariance matrix  $R$  computed by the Jacobi method are  $\lambda_1 \geq \lambda_2 \geq \dots \geq \lambda_p$ . The corresponding feature vectors are  $E_1, E_2, \dots, E_p$ , and the conversion matrix is  $A = E'$ .

**Step 3:** According to the eigenvalues of the covariance matrix, the variance contribution rate of the principal components is calculated, and the cumulative variance contribution rate is obtained. Variance contribution rate  $\eta_k$  of the first principal components and cumulative variance contribution rate  $\xi_m$  of the former  $m$  ( $m < p$ ) principal components  $P_1, P_2, \dots, P_m$  can be calculated as follows:

$$\eta_k = \lambda_k / \sum_{k=1}^p \lambda_k, \quad \xi_m = \sum_{k=1}^m \lambda_k / \sum_{k=1}^p \lambda_k \quad (3)$$

**Step 4:** The number of principal components is determined by the cumulative variance contribution rate.  $M$  principal components are usually considered, and the condition is that the cumulative contribution rate of their variances exceeds 80% [8, 7]. The sample information corresponding to the former  $m$  principal components contains the vast majority of information that can be provided by the  $P$  original variables.

## 3.2. BP neural network and GA

### 3.2.1. BP neural network

BP neural network [9, 13], which possesses a strong nonlinear mapping ability, is a multilayer feed-forward neural network based on an error BP algorithm. It can be used for the prediction of a nonlinear system and applied to the prediction of gas quantity emitted from the coal face. The steps of the BP neural network are as follows. First, the signal passes from the input to the output layer, and the output value and desired error are obtained. Second, the output error is transmitted from the output to the hidden and input layers, and the gradient descent function is used to adjust the weight of each neuron layer. The output value is obtained again, and the cycle is repeated until the output error achieves the desired results.

BP neural networks can effectively deal with complex nonlinear problems in fuzzy prediction. However, they possess disadvantages, such as slow convergence rate, falling easily into a local minimum, and the likelihood of fluctuations and oscillations when approaching the optimum [6, 4]

### 3.2.2. GA

GA, which is based on natural selection and genetic mechanisms, achieves population evolution through selection, crossover, and mutation and produces global optimal values [1]. Given the characteristics of local adjustments in BP neural network and the complexity of nonlinear problems,

several defects exist (e.g., falling easily into the local minimum and slow convergence). GA and BP neural network were combined in this study to overcome these defects.

By using GA to optimize the weights and thresholds of the BP neural network, the performance of the BP neural network can be effectively improved. The steps are as follows:

**Step 1:** Determine the neural network structures: the numbers of nodes in the input and output layers are  $m$  and  $n$ , respectively. Selecting a hidden layer, and the number of nodes is  $q$ . Determine the basic operator of GA and its related operation parameters: the population size is  $p$ , the crossover probability is  $P_c$ , and the mutation probability is  $P_m$  [2].

**Step 2:** Determine the weight of the network and the threshold length. The composition is represented by a vector  $x$ , namely,

$$x = \{v_1, v_2, \dots, v_s, \theta_1, \theta_2, \dots, \theta_T\}^T \quad (4)$$

Where  $v_i$  is the first  $i$  connection weights of the network,  $s$  is the total number of connection weights,  $\theta_j$  is the threshold of the first  $j$  neuron, and  $t$  is the total neuron number in the hidden and output layers.

The total error of the network is defined as:

$$E(x) = \frac{1}{2} \sum_{k=1}^N \sum_{i=1}^n (y_i(k) - o_i(k))^2 \quad (5)$$

Where  $y_i(k)$  and  $o_i(k)$  respectively express the actual and expected outputs of the  $i$  neuron in the output layer of the  $k$  group and  $N$  is the sample group.

According to the optimization goal of GA, the optimal weights and threshold vector  $x$  of the network are searched to minimize the total network error. The GA objective function is defined as

$$\min E(x) = \frac{1}{2} \sum_{k=1}^N \sum_{i=1}^n (y_i(k) - o_i(k))^2 \quad (6)$$

Correspondingly, the fitness function of GA is defined as

$$F(x) = \frac{1}{1 + c + E(x)} \quad (7)$$

Where  $c$  is a non-negative number and satisfies  $c + E(x) \geq 0$ .

**Step 3:** Determine the encoding mode and length. By considering many parameters, efficiency and precision are improved by using a real number to encode. Each individual  $x$  contains all the connection weights and thresholds of a network, where the dimension  $x$  of is the length of coding.

**Step 4:** Generate the initial population and calculate the individual fitness value.

**Step 5:** According to the individual fitness evaluation and testing, GA selection operation is performed. Individuals with the highest adaptation degree in the reserve group are directly copied to the next generation. For other individuals, GA selection operations are performed.

**Step 6:** Execute GA crossover and mutation operations to generate a new generation of population.

**Step 7:** Repeat the GA operation until the evolution of the  $K$  generation (total of the evolutionary algebra). The network weights and thresholds are obtained by decoding the individual with the highest adaptation degree of the  $K$  generation. Total network error  $E(x')$  and its fitness value  $F(x')$  are calculated.

**Step 8:** Implement the convergence criteria and evaluate the results. The convergence criteria are expressed as follows:

$$\min E < \varepsilon \quad (8)$$

Where  $\varepsilon$  represent the total output error of the network. If the convergence criteria are satisfied, a group of solutions corresponding to fitness value  $F(x')$  are the solutions to the problems, which can be obtained by the network to simulate. Otherwise, perform a selection operation in the GA space and return to step 6.

### 3.3. Prediction model of gas emission quantity based on PCA-GA-BP neural network

The problems of slow convergence and falling easily into the local minimum in the application of the BP neural network were overcome by combining PCA and GA for their respective advantages. Thus, the BP neural network was improved in two ways: the sample set and initial weight threshold. The prediction model of gas emission quantity based on PCA-GA-BP was established. First, the input samples of BP neural network were compressed, dimension-reduced, and denoised by PCA. The original samples were replaced by the first principal components as input samples. Second, the BP neural network structure was determined and GA was used to optimize the initial weights and thresholds of the BP neural network. Finally, the prediction of the gas quantity emitted from coal face was realized. Fig. 1 shows the algorithm flow of the model.

## 4. Results Analysis and Discussion

### 4.1. Predictive factors of gas emission quantity

Panbei coal mine in Huainan, China, is a high gas mine with a production capacity of 4.0 Mt/a. The number of workable seams or layers is 14, and the main mineable coal seams are 13-1, 11-2, 8, 5-2, 4-1, 3, and 1. The thickness of each coal seam is 1.64-4.98 m, and the dip angle is  $5^\circ$ - $45^\circ$ . The risk of gas explosion is high due to the complex geological conditions and poor permeability of these coal seams. These factors limit production capacity and affect mine safety and economic benefits. To establish an effective prediction mechanism for gas disasters, 11 factors that influence gas emission from coal faces were proposed synthetically. These 11 factors were: burial depth ( $x_1$ ), thickness ( $x_2$ ), dip angle ( $x_3$ ), gas content in the mining layer ( $x_4$ ), gas content in the adjacent layer ( $x_5$ ), adjacent layer thickness ( $x_6$ ), layer spacing ( $x_7$ ), tensile strength of rock layers ( $x_8$ ),

working face length ( $x_9$ ), propulsion speed ( $x_{10}$ ), and mining intensity ( $x_{11}$ ), which were considered natural, geological, and mining factors of gas emission. In this study, the occurrence conditions and gas emission from coal and rocks in coal mining faces were investigated and monitored, and specific data are shown in Table 4.1. The PCA-GA-BP prediction model of the gas quantity emitted from coal face was established by using the measured parameters as samples.

### 4.2. PCA dimensionality reduction

The sample data in Table 4.1 were normalized and PCA was conducted. The correlation matrix of each factor is shown in Table 4.2. Gas emission quantity was significantly correlated with burial depth, gas content in the mining layer, gas content in the adjacent layer, and layer spacing but was not significantly correlated with thickness, dip angle, and adjacent layer thickness. Gas emission quantity was uncorrelated with tensile strength of rock layers, working face length, propulsion speed, and mining intensity. The correlations between gas emission quantity and the four variables exceeded 60%, and this result indicated that the four variables were the most important parameters affecting gas emission. Several factors in the prediction of gas quantity emitted from the coal face showed a clear correlation with one another, which certainly affected the prediction accuracy of the model. Therefore, it is necessary to analyze the main components of the predictive factors.

The characteristic root of each component, variance contribution rate and cumulative variance contribution rate are shown in Table 4.2. The principal components were selected from large to small, and the feature vectors were selected according to the corresponding eigenvalues. The larger the eigenvalues were, the more important the corresponding principal component data were. The selection criterion for the principal components was that the cumulative variance contribution rate exceeded 80%. Thus, after PCA dimension-reduction processing, the first four principal components, which contained 83.24% of the original data information, were extracted. Most of the information was summed in the forecast factors, so the original 11-dimensional prediction factors were reduced to 4-dimensional prediction factors. The information was consistent with that shown in Fig. 2. The cumulative contribution rate of the first four principal components exceeded 80%, which showed that the four principal components fully reproduced almost all information of the prediction factors for working face gas emission.

According to the fundamentals of PCA, each principal component was linearly transformed. The transformation relationships between the principal components  $Y_1, Y_2, Y_3$  and  $Y_4$  and the predictive factors  $X_1 - X_{11}$  were as follows:

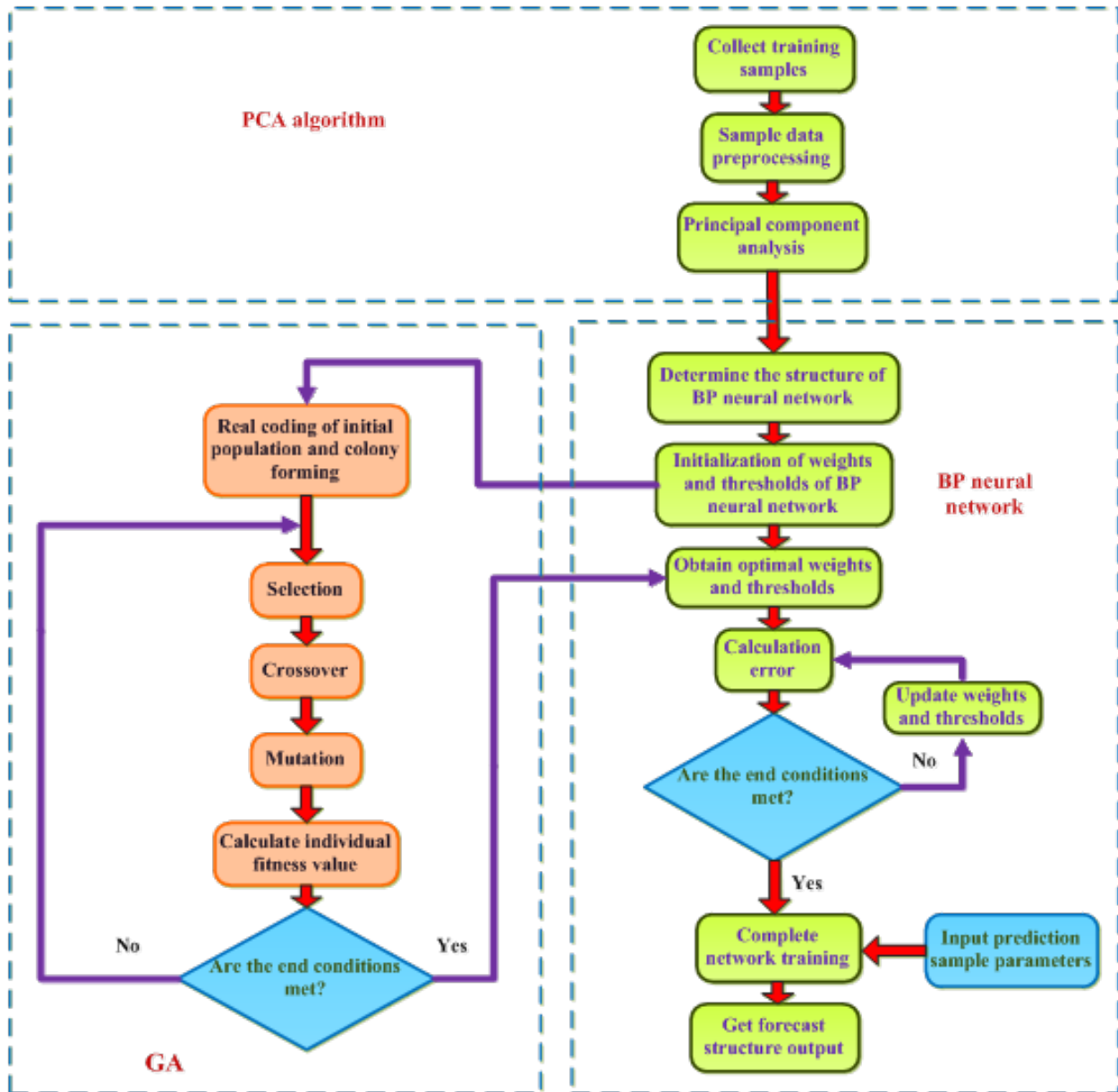


Figure 1: PCA-GA-BP algorithm flow chart

Table 1: Learning sample data

Serial Number	$x_1$ m	$x_2$ m	$x_3$ °	$x_4$ m <sup>3</sup> /t	$x_5$ m <sup>3</sup> /t	$x_6$ m	$x_7$ m	$x_8$ MPa	$x_9$ m	$x_{10}$ m/d	$x_{11}$ t/d	$T$ m <sup>3</sup> /t
1	629	2.5	25	6.34	6.82	2.6	22	3.12	170	3.32	2321	6.34
2	560	1.6	35	5.76	6.14	2.1	24	4.21	180	2.75	1597	5.12
3	412	3.6	23	5.23	4.65	3.8	25	3.86	165	3.12	2480	2.89
4	580	2.2	15	5.97	5.65	2.5	18	4.65	190	4.12	3213	4.87
5	480	2.5	28	6.12	6.45	2.3	23	5.95	210	3.05	2864	3.98
6	460	1.9	40	4.65	5.21	2.1	19	6.43	160	2.97	1675	3.67
7	523	2.1	22	5.89	5.45	1.9	23	6.32	150	3.46	2756	4.22
8	635	3.1	28	5.65	6.12	2.8	28	3.54	220	3.75	3122	6.89
9	604	2.7	32	5.45	5.75	2.9	27	4.35	180	3.06	1875	7.12
10	590	2.5	10	6.21	5.98	2.4	26	6.87	195	4.23	3654	6.19
11	420	3.4	12	4.43	5.32	3.8	21	4.75	210	4.32	3852	3.52
12	654	1.7	26	6.27	6.23	1.9	26	4.86	190	3.54	2642	6.98
13	543	1.9	21	4.35	5.21	2.4	20	5.34	170	3.19	2861	5.34
14	612	2.4	34	5.64	5.78	2.8	28	3.87	200	2.56	1980	5.87
15	439	1.8	17	3.95	4.86	2.1	18	4.86	220	3.87	2987	3.04
16	424	2.6	21	4.23	4.49	2.8	17	3.87	210	3.21	2435	2.89
17	567	2.8	19	4.69	4.89	3.2	24	5.87	170	3.96	2289	5.34
18	650	1.7	27	6.23	5.76	2.0	28	6.12	190	3.12	3142	6.42
19	490	3.4	22	4.34	5.05	3.9	23	4.34	180	3.64	2643	3.98
20	570	2.4	18	5.62	6.21	2.7	21	6.34	220	4.12	2176	6.43

Table 2: Pearson's correlation coefficient matrix of each predictive factor

Serial	$x_1$	$x_2$	$x_3$	$x_4$	$x_5$	$x_6$	$x_7$	$x_8$	$x_9$	$x_{10}$	$x_{11}$	$T$
$x_1$	1											
$x_2$	-0.348	1										
$x_3$	0.196	-0.289	1									
$x_4$	0.699	-0.247	0.163	1								
$x_5$	0.684	-0.268	0.221	0.812	1							
$x_6$	-0.382	0.923	-0.279	-0.422	-0.398	1						
$x_7$	0.615	0.139	0.315	0.551	0.396	0.042	1					
$x_8$	-0.019	-0.352	-0.199	0.097	0.000	-0.399	-0.064	1				
$x_9$	-0.019	0.092	-0.277	-0.069	0.164	0.048	-0.052	-0.155	1			
$x_{10}$	-0.048	0.279	-0.847	-0.113	-0.057	0.234	-0.253	0.270	0.339	1		
$x_{11}$	-0.072	0.222	-0.751	0.027	-0.031	0.109	-0.035	0.187	0.360	0.662	1	
$T$	0.949	-0.231	0.168	0.628	0.695	-0.273	0.635	0.013	0.061	0.015	-0.085	1

Table 3: Principal component characteristic value, variance contribution rate, and cumulative contribution rate

Principal Component	Initial Eigenvalue			Extraction Square and Loading		
	Characteristic Root	Variance Contribution Rate, %	Cumulative Variance Contribution Rate, %	Characteristic Root	Variance Contribution Rate, %	Cumulative Variance Contribution Rate, %
1	3.707	33.699	33.699	3.707	33.699	33.699
2	2.495	22.567	56.379	2.495	22.567	56.379
3	1.932	17.567	73.946	1.932	17.567	73.946
4	1.022	9.292	83.239	1.022	9.292	83.239
5	0.597	5.430	88.668			
6	0.466	4.233	92.901			
7	0.419	3.806	96.706			
8	0.158	1.438	98.144			
9	0.099	0.899	99.043			
10	0.070	0.638	99.681			
11	0.035	0.319	100			

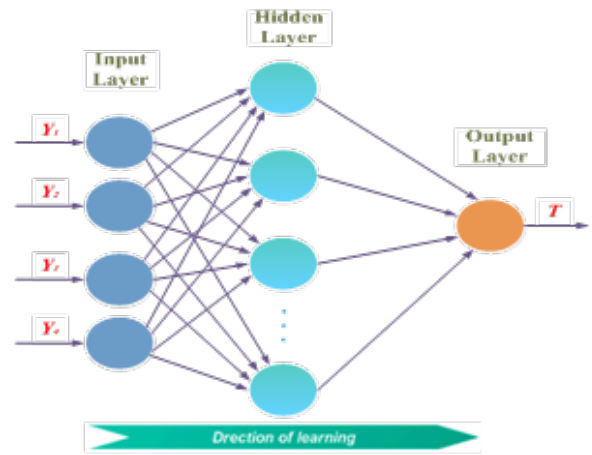
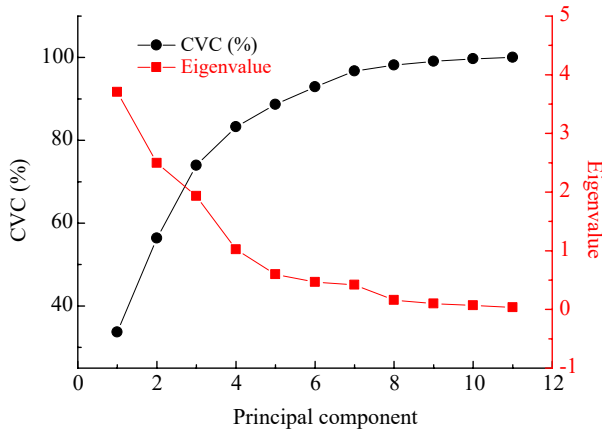


Figure 2: Eigenvalues and cumulative variance contribution rates of different principal components

Figure 3: Three-layer BP neural network model

Table 4: Calculated data of the principal components

Serial Number	$Y_1$	$Y_2$	$Y_3$	$Y_4$	$T, m^3/t$
1	0.9387	0.1012	0.9409	-0.4420	6.34
2	1.4405	-1.0173	-0.2397	-0.7319	5.12
3	-1.0373	-1.3421	1.3690	1.2563	2.89
4	-0.3576	1.0813	-0.5151	-0.3266	4.87
5	0.5061	0.3948	-0.1501	-0.6367	3.98
6	0.4904	-1.7613	-1.7245	0.6062	3.67
7	0.4212	0.1276	-1.1114	1.8088	4.22
8	0.2269	0.7889	1.7742	-1.0943	6.89
9	0.7169	-0.7926	1.0317	0.2720	7.12
10	-0.1359	2.1789	-0.1822	1.2371	6.19
11	-2.1361	0.8002	0.6441	-0.2005	3.52
12	1.2508	0.7995	-0.0910	-0.2269	6.98
13	-0.2275	-0.4167	-1.1415	0.3200	5.34
14	1.0560	-0.8669	1.1737	-0.7185	5.87
15	-1.1234	0.0906	-1.6324	-1.7305	3.04
16	-1.2462	-1.1104	-0.5903	-1.5451	2.89
17	-0.6601	-0.1657	0.0378	1.5762	5.34
18	1.2088	0.8038	-0.2832	0.5997	6.42
19	-1.2525	-0.7261	1.0535	0.6212	3.98
20	-0.0797	1.0322	-0.3638	-0.6445	6.43

$$Y_1 = 0.197X_1 - 0.166X_2 + 0.182X_3 + 0.198X_4 + 0.188X_5 - 0.181X_6 + 0.139X_7 + 0.016X_8 - 0.062X_9 - 0.155X_{10} - 0.124X_{11}$$

$$Y_2 = 0.17X_1 - 0.027X_2 - 0.256X_3 + 0.192X_4 + 0.191X_5 - 0.082X_6 + 0.065X_7 + 0.145X_8 + 0.176X_9 + 0.286X_{10} + 0.295X_{11}$$

$$Y_3 = 0.137X_1 + 0.37X_2 + 0.046X_3 + 0.124X_4 + 0.121X_5 + 0.338X_6 + 0.327X_7 - 0.321X_8 + 0.063X_9 - 0.03X_{10} + 0.006X_{11}$$

$$Y_4 = 0.042X_1 + 0.172X_2 - 0.104X_3 + 0.131X_4 - 0.191X_5 + 0.144X_6 + 0.289X_7 + 0.476X_8 - 0.738X_9 + 0.075X_{10} + 0.049X_{11}$$

According to the initial sample data and the calculation formula, these data were analyzed by PCA. The results shown in Table 4 were then used as the input data of the GA-BP neural network.

### 4.3. Construction and testing of the GA-BP model

#### 1. Structural design of the BP neural network

According to the results of PCA, the dimensions of the input samples of the BP neural network were 4. Therefore, the four prediction factors were used as input nodes for the BP neural network. Gas emission data from the coal face were used as the output node of this network, and one output node was set. Tangsig and purelin functions were selected as the activation function of the hidden and output layers of the BP neural network, respectively, and trainlm function was used in the network-training algorithm. Changes in the number of hidden layers and hidden nodes can affect network performance. As the number of hidden layer nodes increases, network complexity increases. Therefore, a three-layered BP neural network model was selected, and circular iteration was used to determine the optimal network structure. Modeling was performed 30 times in each network structure variation to determine the best hidden-layer node number. Given that the error was minimal when the hidden-layer neuron number was 12, this number was set to 12. The BP neural network prediction model was constructed with 4-12-1. The topology of the BP neural network is shown in Fig. 3.

#### 2. Optimization of the initial weight and threshold values of GA.

Before network training, GA was used to obtain the initial weights and thresholds. By using MATLAB, the parameters were set as follows: population size and genetic algebra were set to 40 and 50, respectively, and crossover and mutation rates were set to 0.7 and 0.01, respectively. The optimal initial weight and threshold values of the BP neural network were obtained.

#### 3. Network training and testing

According to certain rules, the initial weights and thresholds for genetic optimization were inputted into the BP neural network. Sixteen groups of samples (1-16) were trained to obtain the desired error, and the network was tested with four sets of samples (17-20).

Network training parameters were set to goal=0.02 and lr=0.0001. The optimization process for the initial weight

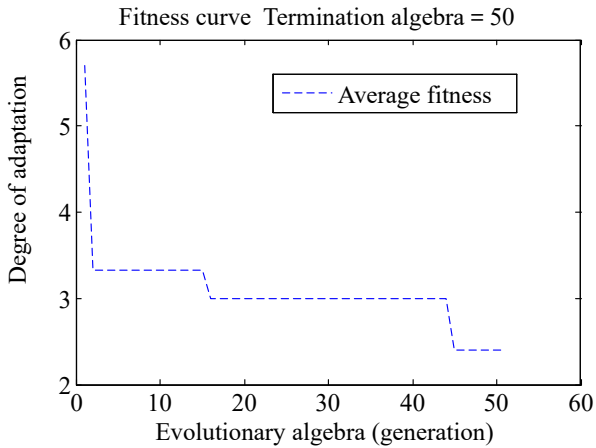


Figure 4: Fitness curves of genetic optimization

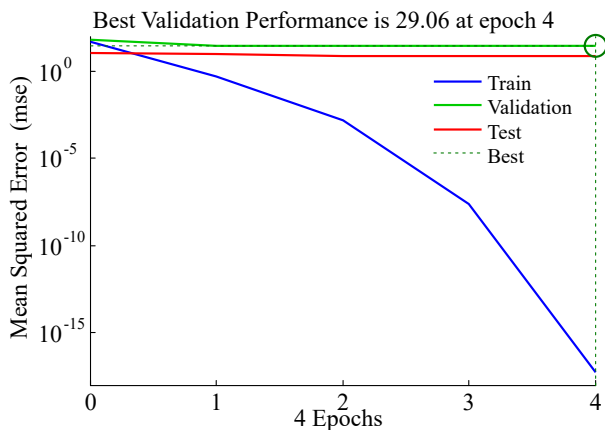


Figure 5: Mean square error curve of the training process

and threshold of the neural network is shown in Fig. 4. The average and optimal fitness values had a good fit and maintained stability after 50 generations. Fig. 5 shows the mean square error curve of the training process. When the training times reached 4, the mean square deviation was  $10^{-4}$ . The smaller the mean square deviation was, the closer the predicted value was to the expected value; however, the corresponding training times increased, which affected the network training speed, and the model might even fall into a death cycle. Comprehensive consideration combined with the prediction results showed that the mean square deviation of  $10^{-4}$  guaranteed the accuracy of the prediction results and did not affect the rapidity of the training process. Therefore, the gas quantity emitted from the coal face was predicted quickly and accurately.

Considering that some randomness existed in the training process, the training results were tested to ensure their accuracy. The linear fitting results of the output value and the expected value are shown in Fig. 6. The correlation coefficient ( $R$ ) was 0.9988, and the fitting degree was close to 1. Compared with the BP model ( $R=0.7916$ ) and the GA-BP

model ( $R=0.9134$ ), the optimized model had higher accuracy. The network output value was close to the expected value, and the tracking effect was improved.

Table 4.3 shows the predicted results obtained from the PCA-GA-BP prediction model. The predicted results for the four groups of working faces were 5.44, 6.32, 3.89, and 6.62. The relative errors of the predicted output were all controlled within 5% and were significantly reduced by the not-principal component analysis. The maximum relative error (MRE) of the PCA-GA-BP model was 3.02%. Compared with that of the BP model (MRE=10.12%) and GA-BP model (MRE=6.45%), the MRE of the optimized model was reduced by 70.2% and 53.2%, respectively. The neural network model after PCA performed better than the standard BP model and GA-BP model in terms of forecasting precision.

## 5. Conclusions

To improve the prediction precision of gas emission quantity and assess the performance of the prediction model, a novel predictive model based on PCA-GA-BP neural network was established in this study. The proposed model was applied to the gas emission prediction of Panbei Coal Mine in Huainan, China. The following conclusions were derived.

1. The PCA method helps deal with the collinearity problems between indexes and improves the prediction accuracy and efficiency; the more indexes there are, the better the superiority is.
2. Gas emission quantity is significantly correlated with burial depth, gas content in the mining layer, gas content in the adjacent layer, and layer spacing. However, it has no significant correlation with the other variables. Geological factors are the main factors affecting the gas emission quantity.
3. Compared with the BP neural network, the combination of GA and BP neural network exerts a better effect on regression prediction of nonlinear problems, and the effect has a significantly positive correlation with sample size and discreteness.
4. The PCA-GA-BP model has higher prediction accuracy and better comprehensive performance than the BP and GA-BP models. This study provides a new method for accurately predicting gas quantity emitted from the coal face.

The proposed method can accurately reflect the nonlinear characteristics and regularity of gas emission quantity and achieve an ideal prediction effect. The method is adaptable and operable. This study also provides convenient and accurate technical support for the prevention and control of mine gas disasters. However, the proposed model does not consider the influence of sample representativeness on prediction accuracy. The amount of gas emission sample data on different areas and different mines should be increased in future studies to further enhance prediction precision.

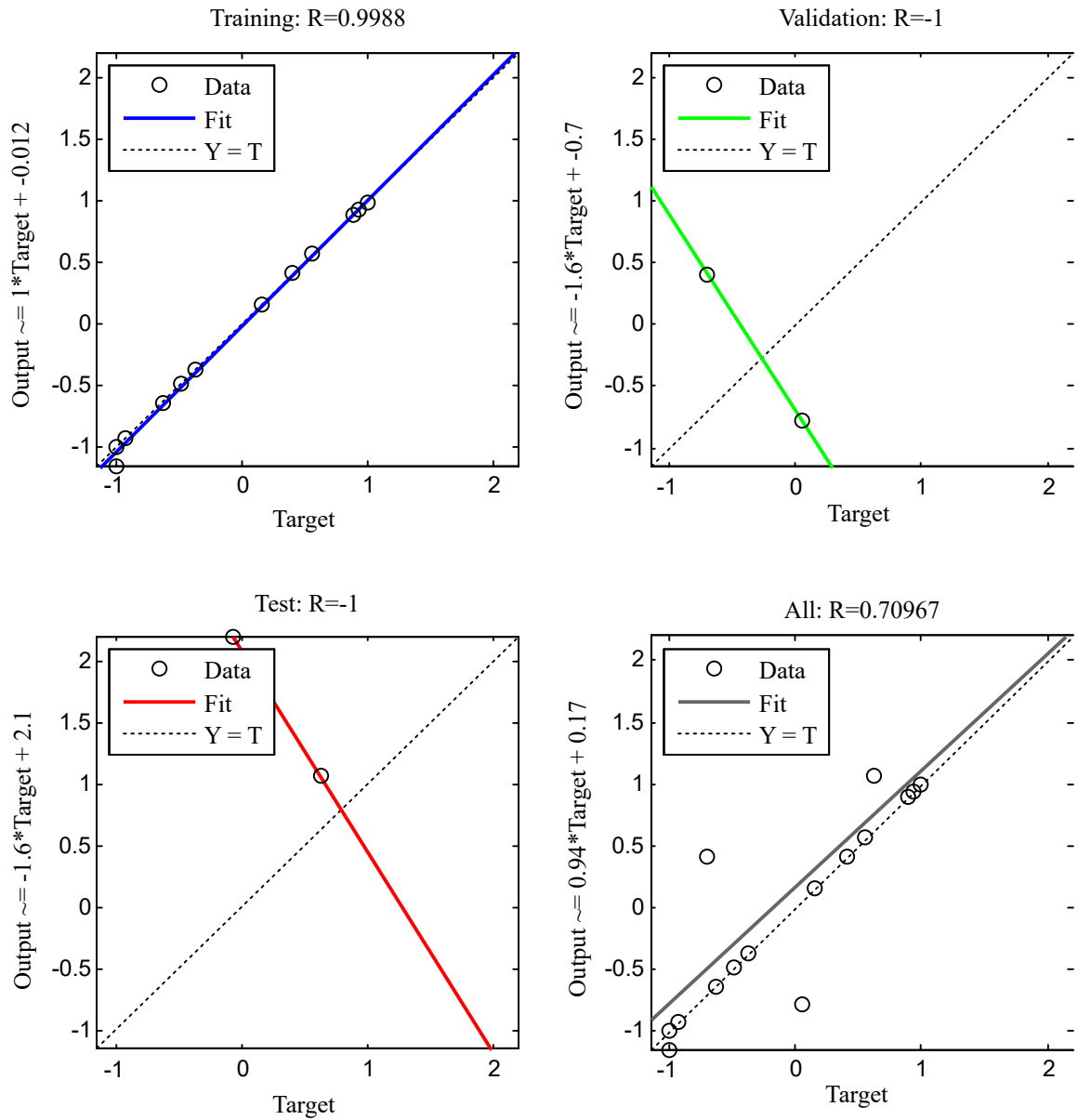


Figure 6: Linear fitting results of the training process: (a) result of the training error, (b) result of the validation error, (c) result of the test error, and (d) results of all errors

Table 5: Prediction results

Serial Number	Measured Value, $m^3/t$	BP		GA-BP		PCA-GA-BP	
		Predicted Value, $m^3/t$	Relative Error, %	Predicted Value, $m^3/t$	Relative Error, %	Predicted Value, $m^3/t$	Relative Error, %
17	5.34	5.87	9.98	5.67	6.24	5.44	1.91
18	6.42	6.74	4.92	6.63	3.29	6.32	1.50
19	3.98	3.78	5.03	3.87	2.69	3.89	2.01
20	6.43	7.08	10.12	6.85	6.45	6.62	3.02

## Acknowledgement

This study was supported by the National Natural Science Foundation of China (No. 51674009, 11472008, 51504009) and the Natural Science Foundation of Anhui Higher Education Institutions of China (No. KJ2016A829).

## References

- [1] Amir Hossein Abolmasoumi and Somayeh Khosravinejad. Chaos control in memristor-based oscillators using intelligent sliding mode control. *Journal of Engineering Science & Technology Review*, 8(2), 2015.
- [2] Zohre Fasihfar and Javad Haddadnia. Designing a fuzzy rbf neural network with optimal number of neuron in hidden layer and effect of signature shape for persian signature recognition by zernike moments and pca. In *Web Information Systems and Mining (WISM), 2010 International Conference on*, volume 1, pages 188–192. IEEE, 2010.
- [3] Lü Fu, Bing LIANG, Wei-ji SUN, and Yan WANG. Gas emission quantity prediction of working face based on principal component regression analysis method [j]. *Journal of China Coal Society*, 1:027, 2012.
- [4] Yuyang Gao, Chao Qu, and Kequan Zhang. A hybrid method based on singular spectrum analysis, firefly algorithm, and bp neural network for short-term wind speed forecasting. *Energies*, 9(10):757, 2016.
- [5] Liu Gaofeng, Wang Huaxi, and Song Zhimin. Study on the mine gas emission rate prediction based on gas geology and grey theory. *International Journal of Earth Sciences and Engineering*, 9(1):327–332, 2016.
- [6] Uneb Gazder and Nedal T Ratrou. A new logit-artificial neural network ensemble for mode choice modeling: a case study for border transport. *Journal of Advanced Transportation*, 49(8):855–866, 2015.
- [7] Na Lin, WN Yang, and Bin Wang. Hyperspectral image classification on kmnf and bp neural network. *Computer Eng. Design*, pages 2774–2777, 2013.
- [8] SHI Long-qing, TAN Xi-peng, WANG Juan, et al. Risk assessment of water inrush based on pca-fuzzy-pso-svc. *Journal of China Coal Society*, 1:167–171, 2015.
- [9] Fangcheng Lü, Chunxu Qin, et al. Particle swarm optimization-based bp neural network for uhv dc insulator pollution forecasting. *Journal of Engineering Science & Technology Review*, 7(1), 2014.
- [10] Klaus Noack. Control of gas emissions in underground coal mines. *International Journal of Coal Geology*, 35(1):57–82, 1998.
- [11] Kotaro Ohga, Sohei Shimada, and Eiji Ishii. Gas emission prediction and control in deep coal mines. *Mineral Resources Engineering*, 9(02): 239–254, 2000.
- [12] Sahan A Ranamukhaarachchi, Ramila H Peiris, and Christine Moresoli. Fluorescence spectroscopy and principal component analysis of soy protein hydrolysate fractions and the potential to assess their antioxidant capacity characteristics. *Food chemistry*, 217:469–475, 2017.
- [13] Luo Ronglei, Liu Shaohua, and Su Chen. Garment sales forecast method based on genetic algorithm and bp neural network. *Journal of Beijing University of Posts and Telecommunications*, 37(4):39–43, 2014.
- [14] Abouna Saghafi. A tier 3 method to estimate fugitive gas emissions from surface coal mining. *International Journal of Coal Geology*, 100: 14–25, 2012.
- [15] Bouhouche Salah, Mentouri Zoheir, Ziani Slimane, and Bast Jurgen. Inferential sensor-based adaptive principal components analysis of mould bath level for breakout defect detection and evaluation in continuous casting. *Applied Soft Computing*, 34:120–128, 2015.
- [16] Shi Shiliang, Song Yi, He Liwen, and Z Chuanqu. Research on determination of chaotic characteristics of gas gush based on time series in excavation working face of coal mine. *Journal of China Coal Society*, 31(6):58–62, 2006.
- [17] Manwendra K Tripathi, PP Chattopadhyay, and Subhas Ganguly. Multivariate analysis and classification of bulk metallic glasses using principal component analysis. *Computational Materials Science*, 107:79–87, 2015.
- [18] Di-Yuan Tzeng and Roy S Berns. A review of principal component analysis and its applications to color technology. *Color Research & Application*, 30(2):84–98, 2005.
- [19] Qi-jun Wang and Jiu-long Cheng. Forecast of coalmine gas concentration based on the immune neural network model. *Journal of the China Coal Society*, 33(6):665–669, 2008.
- [20] Xiao-Lu WANG, Jian LIU, and Jian-Jun LU. Gas emission quantity forecasting based on virtual state variables and kalman filter. *Journal of China Coal Society*, 36(1):80–85, 2011.
- [21] Chun-rong WEI, Yan-xia LI, Jian-hua SUN, Hong-wei MI, and Jun LI. Gas emission rate prediction in coal mine by grey and separated resources prediction method. *Journal of Mining & Safety Engineering*, 4: 029, 2013.
- [22] Xiaoheng Yan, Hua Fu, and Weihua Chen. Prediction of coal mine gas emission based on markov chain improving iga-bp model. *Computer Modelling and New Technologies.*, 18(9):491–496, 2014.
- [23] BAI Yun-xiao. Research on coal mine gas emission forecasting model based on neural network algorithm. *Coal Technology*, 11:050, 2012.
- [24] HQ Zhu, WJ Chang, and Bin Zhang. Different-source gas emission prediction model of working face based on bp artificial neural network and its application. *Journal of China Coal Society*, 32(5):504–508, 2007.